The Journal of the Korean Society of Oceanography
Vol. 31, No. 4, pp. 173-182, December 1996

Injection of an Intermediate Fluid into a Rotating Cylindrical Container Filled with Two-layered Fluid

JUNGYUL NA AND BYONG JUN HWANG
Dept. of Earth & Marine Sciences, Hanyang University, Ansan, 425-791, KOREA

A median-density fluid was injected into the upper layer of a two-layered fluid in a rotating cylindrical container. Several sets of the top and bottom boundary configurations were employed and the flow pattern of each layer including the injected fluid was observed to determine the factors that affect the path of the injected intermediate fluid. The axisymmetric path of the intermediate fluid when the upper layer had a free surface, changed into the asymmetric path with bulged-shape radial spreading whenever either the upper layer or the lower layer had β-effect. The internal Froude number that controls the shape of the interface turned out to be the most important parameter that determines the radial spreading in terms of location and strength. When the upper and lower layer had the β-effect, convective overturning produced anticyclonic vortices at the frontal edge of the intermediate fluid, and that could enhance the vertical mixing of different density fluids. The intermediate fluid did not produce any topographic effect on the upper-layer motion during its spreading over the interface, since its thickness was very small. However, its anticyclonic motion within the bulged-shape produced a cyclonic motion in the lower layer just beneath the bulge.

INTRODUCTION

In recent years laboratory experiments especially those focused on the kinematics and dynamics of ocean convection have been carried out (Marshall, Whitehead and Yates, 1994; Fernando, Chen and Boyer, 1991; Maxworthy and Narimousa, 1994). In these experiments, efforts have been concentrated on determining the size and velocity scales of baroclinic vortices generated by surface cooling or by dense surface of saline water of a rotating tank. These are studies of rotating convection and are mainly concerned with transient behavior of dense water which is mixed and sinks and spreads during its descent. In laboratory experiments, the end-state of the convective process in a homogeneous tank indicates that the convective fluid resides in Rossby-radius-scale eddies (Marshall *at el.*, 1994). However, all laboratory experiments of ocean convection have been carried out in a homogeneous or in a weakly stratified fluid. In fact, it is very rare to find a laboratory experiment of two-layered fluid concentrated on the upper layer motion driven by the lower layer. However, mechanically driven two-layered motions in terms of baroclinic instability (Hart, 1972) and wind-driven circulation modelling (Krishnamurti and Na, 1978) are a few examples of laboratory experiment which were dealt with two-layered fluid.

In an semi-enclosed sea such as the East Sea, winter time convective processes have been observed off the Siberian Coast between 40° and 43°N west of 136°E (Senjyu and Sudo, 1994). The newly formed upper portion of the Japan Sea Proper water (UJSPW) sinks to the isopycnal surface of its own potential density and advected southward to southwestward. This water is mixed vertically with overlying and underlying waters and the thickness of more than 400 m region is found off the Siberian Coast in winter and in summer, the region with thickness of 300 m or more extends further south from the Siberian Coast. If the final state of many convective processes form a new water mass in two-layered ocean, this water mass becomes a third water which has a median density. When this water mass moves the overlying water mass (upper layer)

The study was Supported by the Academic Research Assistance Funds (Fishery and Marine), Ministry of Education in 1995.

as well as the underlying water (lower layer) are affected by the motion of the third water mass. The interaction between three-layered fluid via geostrophic adjustment or by baroclinic instability will be very interesting subjects.

Now consider a two-layered ocean which is subject to wind-stress and a local buoyancy loss from its upper surface. When there is no wind stress on the sea surface, the local negative buoyancy would initiate convective overturning and the cooled surface water would sink until it reaches an equilibrium depth, and spreads out thereafter. When the wind stress is imposed upon in addition to the negative buoyancy, the vertical mixing will be enhanced and the sinking of cooled water will be affected by a large scale wind-driven flow. In particular for a two-layered ocean, if the cooled water reaches the interface and spreads out it may form an intermediate water. As the volume of the intermediate water increases due to continuous mechanical (wind) and thermal (cooling) forcing, the upper layer as well as the lower layer may feel the irregular interface and adjust geostrophically. For example, when a dense fluid is locally injected into a side-wall layer, located at the north, of rapidly rotating homogeneous lighter fluid contained in f- or β-plane, it flows around the rim of the bottom and produces local topographic effect on the homogeneous flow (Na and Hwang, 1995). In their experiment, a large scale flow of homogeneous fluid is generated by denser source fluid that produces vertical motion of the interior flow, that is, via vortex-tube stretching. Thus dual effects of wind-stress and local cooling at the sea surface can be simulated in a laboratory experiment by injection of an intermediate water into a two-layered rotating fluid. Incidently, the area of winter cooling of the East Sea is located in the northern part which is also under strong wind forcing with positive wind-stress curl (Na *et. al.*, 1992).

Previous experiments on the two-layered fluid (Na and Choi, 1993) have been specifically directed toward understanding the response of upper-layer flow when the lower layer is driven by the source, and found that the interface tilting was the major factor in controlling the upper-layer motion. In the laboratory model of rotating two-layered ocean which is subject to dual forcing, the wind stress (actually effect of positive wind stress curl) is simulated by external source into the upper layer, and the local buoyancy loss can be simulated by making the source fluid denser than the upper-layer fluid but lighter than the lower-layer fluid.

Since the source fluid does not mix with either the upper- or lower-layer fluid, it eventually flows along the interface as gravity current. The goal of this experimental study is to find the controlling factor or factors that govern the path of the source fluid (will be called an intermediate fluid hereafter), and also to find interactions between the upper- or lower-layer flow and the intermediate fluid. For this purpose various configurations of upper and lower boundaries are employed to simulate f- and β-planes and this is very common pratice to investigate vorticity dynamics of layered fluid (Matsuura, 1995).

METHOD OF EXPERIMENT

The experimental apparatus is the same as the one previously used for injection of an external fluid into a rigidly rotating fluid in cylindrical container (Na *et. al.*, 1993. 1995) (Fig. 1). The position of injection inlet is located at the mid-depth of the corresponding upper-layer fluid. When the upper layer has a free surface, the mean depth of the upper layer has been kept 3.5 cm. However, when an inclined rigid surface (β-surface) is replaced by the free surface, the mean depth becomes less than 3.5 cm. The mean depth of the lower layer is always 8.5 cm regardless of boundary conditions.

As shown in Table 1, for flow visualization thymol blue solution was used. For example, in order to visualize the motion in the lower layer, a proper amount of sugar was dissolved in the thymol blue solution to have density difference in O (5×10^{-3}), while transparent distilled-water of upper layer provides a relatively sharp interface without significant diffusion at the interface. The most well-defined interface is obtained when the lower layer of starch solution supports the upper layer of thymol blue or distilled water.

Table 1. The workin fluids for the flow visualization of each layer

	upper-alyer fluid	lower-layer fluid	intermediate fluid
observation of intermediate flow patterns	distilled water	starch solution (15 g/3 *l*)	thymol bule solution(1 g/800 m*l*) (with NaOH)
observation of upper-layer motion	thymol bule solution (0.1 g/3 *l*)	starch solution (15 g/3 *l*)	starch solution (1 g/800 m*l*)
observation of lower-layer motion	distilled water	thymol bule solution(3*l*) (with sugar(15 g))	starch solution (1 g/800 m*l*)
density (g/cm^3)	1.000	1.005	1.001

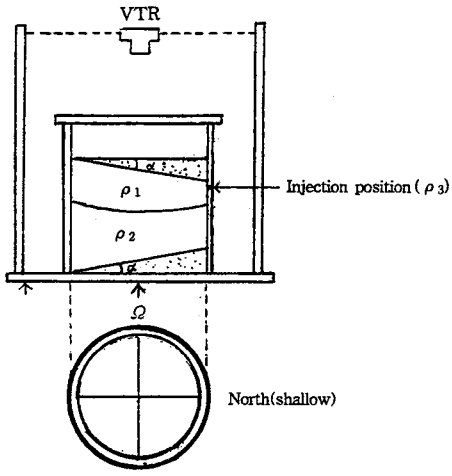

Fig. 1. Geometry of the cylindrical container with top and bottom boundaries of inclined surface. The upper boundary is floating and moves up during the period of injection. The injection position corresponds to the north, i.e., the shallowest depth. VTR is mounted on the rotating frame to record the flow patterns. (tanα=0.1)

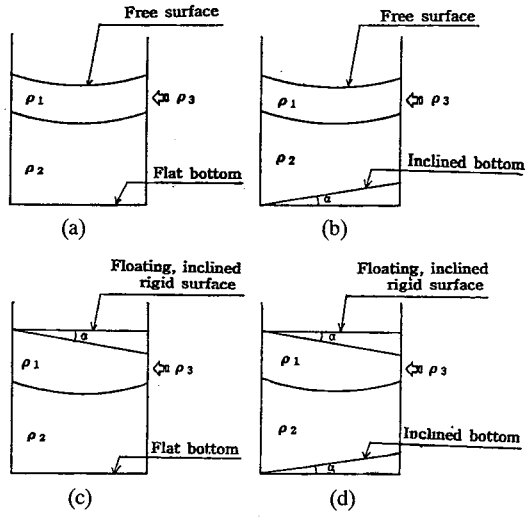

Fig. 2. The geometry of cylindrical container with different boundary conditions. The angle of inclination is the same for both the surface and the bottom. a) free surface and flat bottom (f-f plane) b) free surface and inclined bottom (f-β plane) c) inclined surface and flat bottom (β-f plane) d) inclined surface and inclined bottom (β-β plane)

To trace the path of the intermediate fluid, dyed solution (deep blue color) that was made by adding dense NaOH solution to the thymol blue solution, was used. In this case no significant diffusion of color was observed. As for the boundary conditions at the top and the bottom, four different types of boundary conditions were employed as shown in Fig. 2. In particular, to make both layers feel the β-effect the top boundary is a floating inclined surface which has the same slope as the bottom. In this way the shallowest depth in both layers correspond to the north. In order to avoid any inertial effect of injected fluid, a diffuser was installed at the tip of the inlet. Before the start of injection, two-layered fluid was spun up and this was checked by top-mounted video camera which shows that dyed-lines in the upper layer stay along the electrodes mounted across the container.

The intermediate fluid was pumped into the middle of the upper layer through a hole placed at the sidewall of the container in the north. The peristaltic pump of precisely controllable injection rate was used and the pumping rate was fixed at 0.04 m/s^{-1}. Most of the experiments were performed with a basic rotation rate of 20 rpm which corresponds to a Rossby number, Ro=U/2ΩL, of O (10^{-3}), where U is the characteristic velocity, Ω is the basic rotation rate and L is

the radius of the container. To change the magnitude of internal Froude number (Fi) $Fi=\Omega^2L/g^*$, where g^* is a reduced gravity, only Ω was varied.

For a given boundary condition, different experiments were carried out to observe motions in each fluid layer. First, to observe the path of the intermediate fluid of dyed solution, the upper layer of distilled water was on top of the layer of starch solution. Second experiment was to observe the upper layer motion, and the upper layer fluid of thymol blue solution was above the lower layer of starch solution. In this case the intermediate fluid was a denser starch solution. Third experiment was to observe the lower-layer motion by using the upper layer of transparent distilled water over the denser thymol blue solution, and the intermediate fluid was the starch solution.

OBSERVATIONS OF THE FLOW PATTERN

For a given boundary condition at the top and the bottom of the container, flow pattern of the intermediate fluid, the upper-layer and the lower-layer motions were observed separately. Dyed intermediate fluid was used to follow its path in the transparent upper layer, and thymol-blue solution for both the upper and the lower layer was used but it produced a less clear pattern compared to the dyed injected fluid.

Fig. 3~6 show the flow patterns which were taken 20 minutes after the start of injection corresponding to four different boundary conditions. In case of free surface and flat bottom (Fig. 3), the path of intermediate fluid was almost circular along the rim of the container. The influx position of the intermediate fluid was located at the north (as seen in Fig 3-a, the position corresponds to the top of the picture). When the fluid entered the upper layer it sank and after entering the interior it deflected to the right due to the Coriolis force. The diffuser installed at the entrance prevented the intrusion into the in-

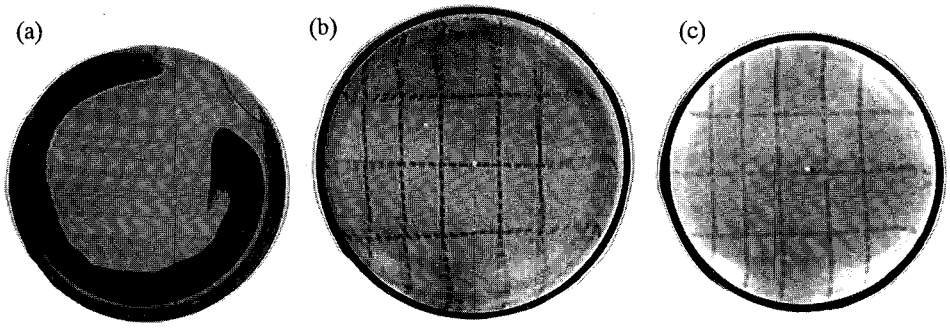

Fig. 3. The flow patterns of the intermediate fluid a), upper layer b) and lower layer c) for the f-f plane geometry. Axisymmetric patterns are prominent in the upper-layer motion and the intermediate flow.

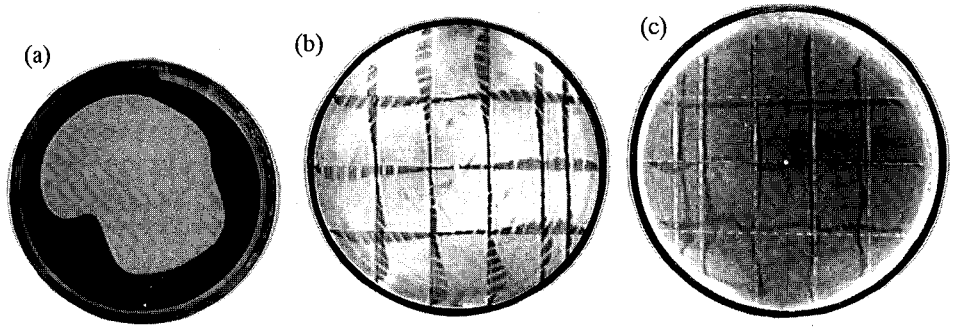

Fig. 4. The flow patterns of the intermediate fluid a), upper layer b) and lower layer c) for the f-β plane geometry. A bulge-shaped radial spreading of the intermediate fluid at the southwestern corner is clearly seen. Axisymmetric upper-layer motion and a local cyclonic motion in the lower layer reflects the position of the bulged-shape fluid.

terior and the sinking motion occurred within the narrow sidewall layer. The width of the intermediate fluid did not increase until it arrived at the East corner and thereafter, slightly increased as it moved along the rim of the container, but the flow was almost axisymmetric. The motion in the upper layer which was driven by the intermediate flow via vortex-tube stretching (counterclockwise rotation) revealed the existence of the axisymmetric circulation (Fig. 3-b). However, the lower layer did not show any appreciable motion compared to the upper one. It was almost motionless during the period of observation indicating that the interfacial stress was indeed negligible (Fig. 3-c). The maximum azimuthal velocity of the intermediate flow was 0.04 cms^{-1} which was twice as large as the upper-layer flow and the lower-layer velocity was observed to be very small with an axisymmetrical cyclonic motion.

For free surface and the inclined bottom condition (Fig. 4), the injected flow pattern no longer axisymmetric. Steady and bulged shape of the intermediate fluid was seen both in the southwestern corner and in the northeastern corner but with weaker strength. The upper-layer flow pattern was almost axisymmetric except the southwestern corner where the southward velocity was weaker compared with that of the eastern side (Fig. 4-b)). The most significant flow pattern influenced by the bulge of the intermediate fluid appeared in the lower-layer motion. The mean width of the bulge was almost same as the internal Rossby radius deformation (~2 cm). In the southwestern corner of the basin, the closed-cell pattern of cyclonic flow was very strong while very weak flow occupied the rest of the basin of the lower layer. Thus, where the intermediate flow was interrupted, there existed a closed-cell type separated flow pattern in the lower layer that might be influenced by both the upper-layer motion and the injected fluid. It was of interest to note that the magnitude of flow speed corresponding to the closed-cell of the lower layer was comparable with that of the upper layer.

When the top of the upper layer was replaced by an inclined rigid surface (β-effect), the path of the intermediate flow was no longer axisymmetric (Fig. 5). Furthermore unlike the narrow width of the flow right after leaving the influx position, radial spreading of the intermediate fluid was very noticeable in the northwestern corner and this may be due to a frictional force produced by the upper lid (Fig. 5-a)). Incidently a false image of the intermediate flow pattern appeared in the picture as a sharp discontinuity of the path of the intermediate fluid in the northwest and in the southeastern corne due to refraction of light by the plastic enforcer mounted on the inclined rigid surface. Striking features were; a wavy pattern of the intermediate fluid around the southeastern corner of the basin, and a sharp turning into the interior near the eastern wall. There was northward flow along the rim boundary of very thin width, though it is not seen clearly in the picture. The wavy pattern consisted of three bulges and not due to the drift of a single bulge; rather the bulges were

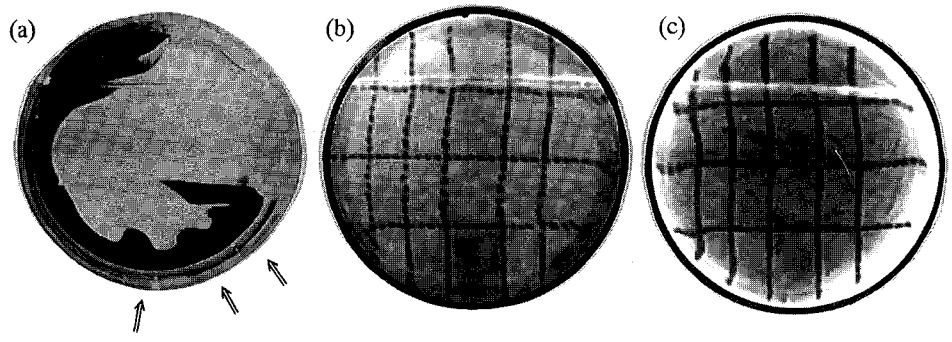

Fig. 5. The flow patterns of the intermediate fluid a), upper layer b) and lower layer c) for the β-f plane geometry. The arrows indicate the positions of generation of bulge-shaped flow.

generated at three different locations indicated by the arrow marks in Fig. (5-a). It was also observed that the azimuthal speed of individual bulge was very much less than the speed of the frontal edge of the intermediate fluid. The upper-layer motion induced by source of the intermediate fluid was not a cyclonic singe-cell which was observed with the free-surface boundary. Rather it consisted of two-cell flow. A broad anticyclonic flow was predominant over the eastern half of the basin while narrower cyclonic flow occupied the southwestern corner of the basin. A wavy dye line across the northern part of the basin was also noticeable. The strongest southward flow existed along the eastern boundary where narrow northward flow of the intermediate fluid was observed. However, in the lower layer, a single-cell cyclonic motion with relatively stronger speed along the rim was observed.

When both top and bottom boundaries were β-planes (Fig. 6), inward spreading of the intermediate fluid around the southeastern corner was prominent. A narrow northward flow along the eastern boundary (not seen clearly in the picture) and broad and diffuse pattern of eastward spreading of the intermediate fluid near the injection point were clearly seen. The bulge shaped flows, which were generated at the positions indicated by arrow marks in figure, showed a relatively slower azimuthal propagation with speed about an half of the β-f plane. In the upper layer a narrow western boundary flow occupied almost western half of the rim boundary. A broad anticyclonic circulation with strong southward eastern boundary flow was also observed. No wavy pattern was seen in the upper layer. However, the flow pattern of the lower layer showed very distinct features such as a anticyclonic circulation occupied the western half of the basin with northward flowing western boundary flow. At the same time a narrow cyclonic circulation existed along the eastern boundary.

DISCUSSION

The two-layered fluid with various upper and lower boundary planes was driven by a median-density fluid. This three-layer motion reveals very complicated interactions with each other. The role of the intermediate fluid in terms of driving the upper layer motion and the influence of upper and lower layer motion on the path of the intermediate fluid are the one of the most important point of this experiment study.

From observations of the flow patterns in each layer the most significant factor that influenced the path of the intermediate fluid was the β-effect. In other words the β-plane, top and bottom boundary conditions, played an important role in controlling the spreading pattern of the intermediate fluid in the form of the radial spreading. Incidently the numerical experiments of evolution of frontal-geostrophic vortices in a two-layered ocean conducted for the f- and β-planes (Matsuura, 1995), show that the vortex on the β-plane radiates Rossby waves to the lower ocean simultaneously with the occurrence

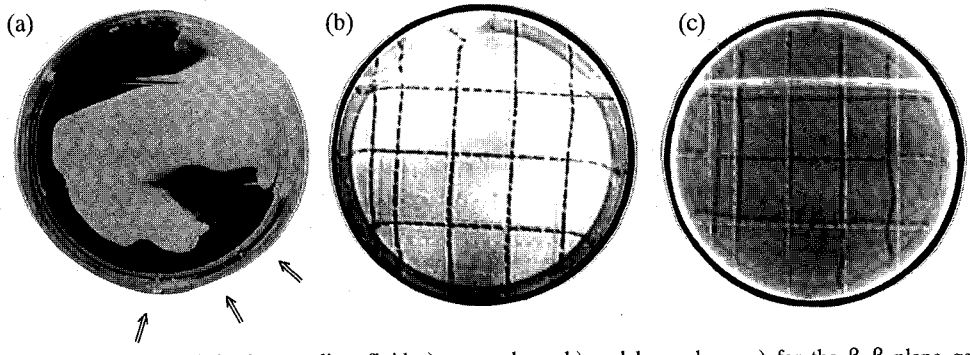

Fig. 6. The flow patterns of the intermediate fluid a), upper layer b) and lower layer c) for the β–β plane geometry. The arrows indicate the positions of generation of bulge-shaped flow.

of baroclinic instability. Almost symmetrical flow along the rim of the container was a prominent pattern of the intermediate fluid when the upper layer had free surface.

With free surface, the upper-layer motion was driven by the denser source fluid such that vortex-tube stretching resulted in cyclonic circulation in the upper layer. Therefore the geostrophic upper layer did not feel the bottom formed by the intermediate fluid. In fact the thickness of the intermediate fluid was observed to be very small. Since the interfacial stress was negligible between the fluids in each layer, the axisymmetric upper-layer motion was not transferred to the lower layer which was almost quiescent. However, underneath the bulged part of the intermediate fluid, a cyclonic motion in the lower layer existed. The bulging was due to radial spreading of the intermediate fluid, and within the bulge anticyclonic motion restricted further radial spreading so as to keep azimuthal spreading of the intermediate fluid along the rim. Therefore, the cyclonic motion of the lower layer could be enhanced by the baroclinic adjustment to the anticyclonic intermediate flow just above it. The width of the intermediate flow when it comes to geostrophic equilibrium was given by Stern (1975) as (L/λ)-tanh $(L/\lambda)=L_o/\lambda$, where L is the width of the intermediate fluid, L_o is the initial width and λ is the Rossby radius deformation. In this experiment λ is very small (about 0.2), so the initially imbalanced state only spreads a small distance in the radial direction before geostrophic balance within about 1.5 sec. Therefore, spreading of the intermediate fluid in bulged shape or in radial direction seems to reflect a gradual increasing of radial pressure gradient by accummulation of the injected fluid along the rim of the injected fluid along the rim of the container.

The β-plane at the bottom would produce a southward western boundary flow if the lower layer felt the cyclonic upper-layer motion. Indeed, there was a southward western boundary flow which merged into the cyclonic motion in the lower layer. Incidently, the anticyclonic motion of the intermediate flow within the bulged shape could change the interface to drive the lower layer into the cyclonic motion via vortex-tube stretching, or *vice versa*. Only in the experiments with f-β plane stronger radial spreading of the intermediate fluid was observed and radial extent of the bulged shape flow remained unchanged even for various rotation rates.

Fig. 7 shows the flow patterns of the intermediate fluid for different internal Froude numbers in the f-β plane. The internal Froude number was changed by changing the basic rotation rate. The distinct bulged shapes appeared only when the internal Froude number, F_i, was in the range $7.47 \leq F_i \leq 9.13$, and they were almost stationary with their average radii close to the internal Rossby radius of deformation of about 2 cm. Previous observations of the axisymmetric upper-layer motions regardless of the upper boundary condition (Figs 4 and 5) suggest that there existed a strong interaction between the bulged-shape intermediate flow and the lower-layer motion. In addition to the radial spreading of the intermediate fluid the radial width of the intermediate flow at the western boundary changed with internal Froude number.

In Fig. 8, the minimum width of the intermediate fluid and the corresponding internal Rossby radius of deformation are plotted against the internal

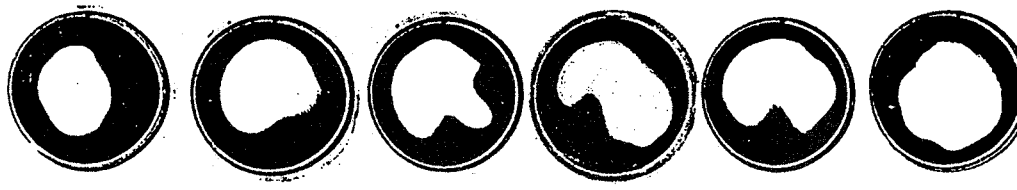

Fig. 7. The flow patterns of the intermediate fluid for different internal Froude number (F_i) for the f-β plane geometry. These pictures were taken at 30 min after the start of the injection. a) 2.07 b) 4.66 c) 7.47 d) 8.28 e) 9.13 f) 12.94

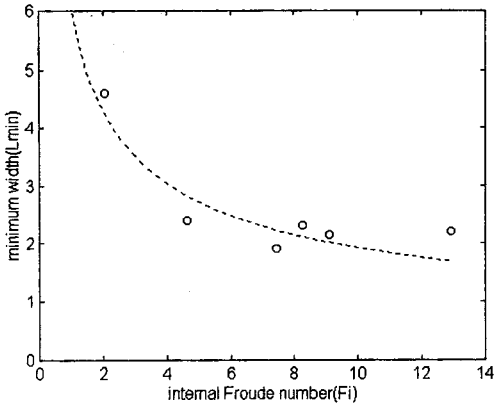

Fig. 8. The minimum width('o') of the intermediate fluid versus internal Froude number (F_i) for the f-β plane geometry. The dotted line corresponds to the internal Rossby radius of deformation.

Froude number, Fi. It is interesting to note that the width approximately coincides with the radius of deformation except the cases of appearance of the bulged-shape flow. In general the radial spreading was always dominant over the eastern half of the basin. But when the upper layer had free surface and the rotation was reduced in half, i.e., decreasing the internal Froude number or increasing the Rossby number, the radial spreading became dominant over the western side (Fig. 9). This could be the result of western intensification in the lower-layer motion due to β-effect, in that a narrower western boundary flow affected the path of the intermediate fluid. For f-f plane geometry, the axisymmetric motion of the intermediate fluid as it approached the north, and accumulation of the intermediate fluid could generate a radial pressure gradient to drive the fluid inward.

When β-effect was imposed on the upper layer, the path of the intermediate flow never formed a closed shape. Rather very strong radial spreading at the east disrupted the continuing path of the fluid toward the north. However a very thin layer existed along the eastern wall, which was not an extension of the azimuthal component of the intermediate flow, but was formed by the anticyclonic motion of the intermediate fluid as it moved inward and changed its direction toward the wall. In the northern part, the radial spreading, which was broader and slower than that in the east, caused the upper layer to move

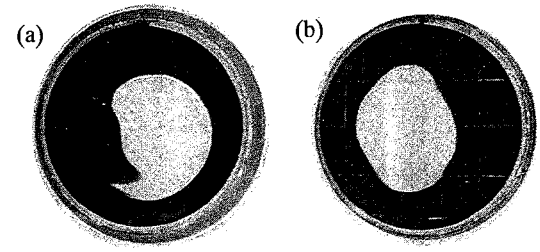

Fig. 9. Flow patterns of the intermediate fluid for f-f plane a), f-β plane b) geometries when the rotation was reduced to 10 rpm.

cyclonically over that part. Actually the upper layer experienced vortex-tube stretching due to the external source of the injected fluid. Therefore it was expected to have northward flowing interior motion and a strong southward flowing western boundary current, i.e., the Sverdrup flow. But the radial spreading or accumulation of the intermediate fluid could change the slope of the interface into "a flat surface" in such a way as to make the upper-layer flow over the intermediate fluid experience the vortex-tube stretching, producing a cyclonic motion. In the upper-layer motions shown in figures 5 and 6 weaker western boundary flow formed a cyclonic motion on top of the intermediate fluid along the western side of the basin. And a broad anticyclonic motion with strong southward eastern boundary flow occupied the rest of the basin. In particular, very strong vertical shear of the eastern boundary flows of the northward intermediate fluid and the southward upper-layer flow were prominent at the eastern wall. Also it should be noted that where the upper-layer flow was convergent, especially near the southeastern corner the radial intrusion of the intermediate flow was very active. Therefore both the vertical shear in the east and the horizontal shear at the frontal edge of the intruding fluid enhanced mixing of the intermediate fluid and the upper-layer fluid to produce a new density-fluid which became heavier than the upper-layer fluid. If the new density-fluid was moved into the interior of the upper layer, convective overturning occurred to produce anticyclonic vortices at the edge of the front (Fig. 10). The diameter of the vortices were almost same as the internal Rossby radius of deformation. The

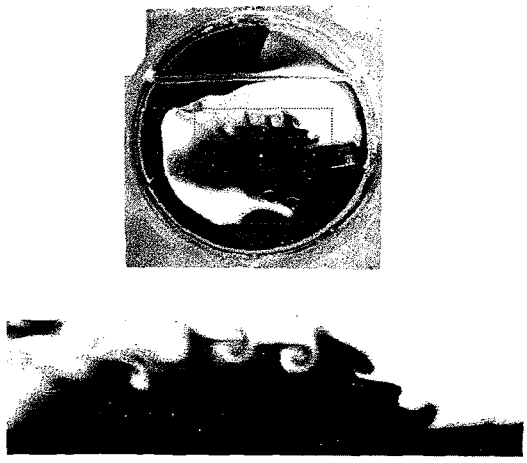

Fig. 10. Anticyclonic vortices that appeared at the edge of the spreading front with mean diameter which coincides with the internal Rossby radius of deformation, 1.8 cm. The photograph was taken 35 min after the start of injection for the β-β plane geometry. The enlarged portion corresponds to the dotted portion in the interior.

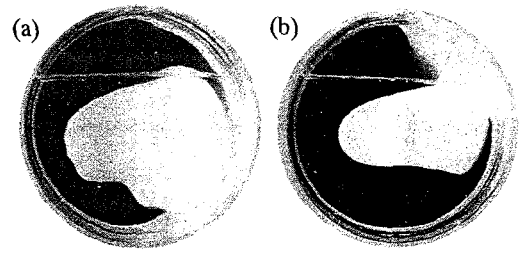

Fig. 11. The flow patterns of the intermediate fluid for the β-f plane a), β–β plane b) geometries for 10 rpm, showing a sharp intrusion along the east, but the direction of the flow was reversed. Compare these with Fig. 5 and 6.

northward intrusion of the intermediate fluid at the eastern wall as well as the eastward spreading at the north were common features of the flow pattern for the β-β plane geometry. But when the rotation rate was reduced to half, in β-f plane (Fig. 11-a) eastward spreading was dominant while in β-β plane, northward flow of the intermediate fluid was well defined (Fig. 11-b).

CONCLUSION

A two-layered fluid in a rotating cylindrical container with four different surface-bottom configurations were subjected to an external source that was heavier than the upper layer but lighter than the lower layer. The external source fluid was injected into the upper layer through a diffusive hole at the side wall after the two-layered fluid had spun-up. Observations of the flow pattern in each layer were carried out by using a colored fluid for the intermediate flow, thymol blue solution for the upper and the lower layer. The path of the intermediate flow was strongly dependent on the boundary condition such that whenever either boundary constituted a β-plane, the axisymmetric path, which always appeared in the f-f plane, changed into an asymmetric pattern. The asymmetric path was mainly due to local radial spreading in the form of bulged wavy pattern or broad radial intrusion toward the interior. The radial width of the intermediate flow at the western boundary as well as the mean radius of the bulged-shape flow were about the same size of the internal Rossby radius of deformation. When the upper layer had the free surface the path of the intermediate fluid did not affect the axisymmetric and geostrophic flow of the upper layer since the intermediate fluid was so thin that the upper layer did not feel any topographic effect. However, whenever β-effect was imposed upon the upper-layer motion, western boundary layer flow in the upper layer induces a strong radial spreading of the intermediate fluid at the position where the upper-layer flow was convergent. The lower layer played an insignificant role in terms of the radial spreading of the intermediate fluid whether the bottom was an f-plane or a β-plane. The most prominent radial spreading occurred when both the upper and lower surfaces were β-planes and at the frontal edge of the radially spreading intermediate fluid, convective overturning of the mixed fluid produced anticyclonic vortices of mean diameter about equal to the internal Rossby radius of deformation. Such convective motions were also observed by Marshall *et al.* (1994) as the end-state of the convective process in a homeogenous rotating fluid.

Thus the most important factor that controls the path of the intermediate fluid was the upper-layer motion which was strongly influenced by the im-

posed boundary condition such as the β-plane. And also the intermediate fluid, when it spreads over the top of the interface, it can modify the interface slope so as to have the upper layer adjust geostrophically and the resultant upper-layer motion eventually affects the path of the intermediate fluid. The intermediate fluid may be regarded as being formed by a final state of winter time convection occuring off the Siberian Coast of the East Sea. In an extreme case, this fluid can be a water which occupies the column of depth of main oceanic thermocline which has a typical vertical thickness of ~1 km, and maintain its thickness without collapsing. Therefore, from the geophysical point of view, the dynamics involving the path of the intermediate fluid and the upper and lower layer motions may reflect the real ocean phenomena in some extent. Experiments in an annulus container with various boundary conditions are presently being constructed to ensure the radial symmetry of the flow. With such an apparatus, the injection can be carried out along the inner rim of the annulus which corresponds to the north in a β-plane. The results of this experiment will be reported in the near future.

REFERENCES

Fernando, J.S.F., R. Chen and D.L. Boyer, 1991. Effects of rotation on convection turbulence. *J. Fluid Mech.*, **228:** 513-548.

Hart, J.E., 1972. A laboratory study of baroclinic instability. *Geophy. Fluid Dyn.*, **3:** 181-209.

Krishnamurti, R. and J.Y. Na, 1978. Experiments in ocean circulation modelling. *Goephys. Astrophys. Fluid Dyn.*, **11:** 13-22.

Marshall, J.C., J.A. Whitehead and T. Yates, 1994. Laboratory and numerical experiments in oceanic convection. In: Ocean Processes in Climate Dynamics: Global and Mediterranean Examples, edited by Malanotte-Rizzoli and Robinson, Kleuver Academic Publishers, 173-201 pp.

Matsuura, T., 1995. The Evolution of Frontal-Geostrophic Vortices in a Two-layered Ocean. *J. Phys. Oceanogr.*, **25:** 2298-2318.

Maxworthy, T. and S. Narimousa, 1994. Unsteady, turbulent convection into a homogeneous, rotating fluid, with oceanographic applications. *J. Phys. Oceanogr.*, **24:** 865-887.

Na, J.Y., et al., 1992. Monthly-mean sea surface winds over the adjacent seas of the Korea Peninsular. *J. Oceanol. Soc. Korea*, **27:** 1-10.

Na, J.Y. and J.Y. Choi, 1993. Laboratory experiment of two-layered fluid in a rotating cylindrical container. *J. Oceanol. Soc. Korea*, **28 (1):** 17-23.

Na, J.Y. and B.J. Hwang, 1995. Injection of a denser fluid into a rotating cylindrical container filled with homogeneous lighter fluid. *J. Oceanol. Soc. Korea*, **30 (4):** 355-364.

Pedlosky, J., 1986. Geophysical Fluid Dynamics. Springer Verlag., NY., 416-426 pp.

Senjyu, T. and H. Sudo, 1994. The Upper Portion of the Japan Sea Proper Water. *J. Ocenogr., Japan*, **50:** 663-690.